

Search for Nonstandard Higgs Bosons Using High Mass Photon Pairs in $p\bar{p} \rightarrow \gamma\gamma + 2 \text{ Jets at } \sqrt{s} = 1.8 \text{ TeV}$

B. Abbott,⁴⁰ M. Abolins,³⁷ V. Abramov,¹⁵ B. S. Acharya,⁸ I. Adam,³⁹ D. L. Adams,⁴⁹ M. Adams,²⁴ S. Ahn,²³ G. A. Alves,² N. Amos,³⁶ E. W. Anderson,³⁰ M. M. Baarmand,⁴² V. V. Babintsev,¹⁵ L. Babukhadia,¹⁶ A. Baden,³³ B. Baldin,²³ S. Banerjee,⁸ J. Bantly,⁴⁶ E. Barberis,¹⁷ P. Baringer,³¹ J. F. Bartlett,²³ A. Belyaev,¹⁴ S. B. Beri,⁶ I. Bertram,²⁶ V. A. Bezzubov,¹⁵ P. C. Bhat,²³ V. Bhatnagar,⁶ M. Bhattacharjee,⁴² N. Biswas,²⁸ G. Blazey,²⁵ S. Blessing,²¹ P. Bloom,¹⁸ A. Boehnlein,²³ N. I. Bojko,¹⁵ F. Borchering,²³ C. Boswell,²⁰ A. Brandt,²³ R. Breedon,¹⁸ G. Briskin,⁴⁶ R. Brock,³⁷ A. Bross,²³ D. Buchholz,²⁶ V. S. Burtovoi,¹⁵ J. M. Butler,³⁴ W. Carvalho,² D. Casey,³⁷ Z. Casilum,⁴² H. Castilla-Valdez,¹¹ D. Chakraborty,⁴² S. V. Chekulaev,¹⁵ W. Chen,⁴² S. Choi,¹⁰ S. Chopra,²¹ B. C. Choudhary,²⁰ J. H. Christenson,²³ M. Chung,²⁴ D. Claes,³⁸ A. R. Clark,¹⁷ W. G. Cobau,³³ J. Cochran,²⁰ L. Coney,²⁸ W. E. Cooper,²³ D. Coppage,³¹ C. Cretsinger,⁴¹ D. Cullen-Vidal,⁴⁶ M. A. C. Cummings,²⁵ D. Cutts,⁴⁶ O. I. Dahl,¹⁷ K. Davis,¹⁶ K. De,⁴⁷ K. Del Signore,³⁶ M. Demarteau,²³ D. Denisov,²³ S. P. Denisov,¹⁵ H. T. Diehl,²³ M. Diesburg,²³ G. Di Loreto,³⁷ P. Draper,⁴⁷ Y. Ducros,⁵ L. V. Dudko,¹⁴ S. R. Dugad,⁸ A. Dyshkant,¹⁵ D. Edmunds,³⁷ J. Ellison,²⁰ V. D. Elvira,⁴² R. Engelmann,⁴² S. Eno,³³ G. Eppley,⁴⁹ P. Ermolov,¹⁴ O. V. Eroshin,¹⁵ V. N. Evdokimov,¹⁵ T. Fahland,¹⁹ M. K. Fatyga,⁴¹ S. Feher,²³ D. Fein,¹⁶ T. Ferbel,⁴¹ H. E. Fisk,²³ Y. Fisyak,⁴³ E. Flattum,²³ G. E. Forden,¹⁶ M. Fortner,²⁵ K. C. Frame,³⁷ S. Fuess,²³ E. Gallas,⁴⁷ A. N. Galyaev,¹⁵ P. Gartung,²⁰ V. Gavrilov,¹³ T. L. Geld,³⁷ R. J. Genik II,³⁷ K. Genser,²³ C. E. Gerber,²³ Y. Gershtein,¹³ B. Gibbard,⁴³ B. Gobbi,²⁶ B. Gómez,⁴ G. Gómez,³³ P. I. Goncharov,¹⁵ J. L. González Solís,¹¹ H. Gordon,⁴³ L. T. Goss,⁴⁸ K. Gounder,²⁰ A. Goussiou,⁴² N. Graf,⁴³ P. D. Grannis,⁴² D. R. Green,²³ H. Greenlee,²³ S. Grinstein,¹ P. Grudberg,¹⁷ S. Grünendahl,²³ G. Guglielmo,⁴⁵ J. A. Guida,¹⁶ J. M. Guida,⁴⁶ A. Gupta,⁸ S. N. Gurzhiev,¹⁵ G. Gutierrez,²³ P. Gutierrez,⁴⁵ N. J. Hadley,³³ H. Haggerty,²³ S. Hagopian,²¹ V. Hagopian,²¹ K. S. Hahn,⁴¹ R. E. Hall,¹⁹ P. Hanlet,³⁵ S. Hansen,²³ J. M. Hauptman,³⁰ C. Hebert,³¹ D. Hedin,²⁵ A. P. Heinson,²⁰ U. Heintz,³⁴ R. Hernández-Montoya,¹¹ T. Heuring,²¹ R. Hirosky,²⁴ J. D. Hobbs,⁴² B. Hoeneisen,^{4,*} J. S. Hoftun,⁴⁶ F. Hsieh,³⁶ Tong Hu,²⁷ A. S. Ito,²³ J. Jaques,²⁸ S. A. Jerger,³⁷ R. Jesik,²⁷ T. Joffe-Minor,²⁶ K. Johns,¹⁶ M. Johnson,²³ A. Jonckheere,²³ M. Jones,²² H. Jöstlein,²³ S. Y. Jun,²⁶ C. K. Jung,⁴² S. Kahn,⁴³ G. Kalbfleisch,⁴⁵ D. Karmanov,¹⁴ D. Karmgard,²¹ R. Kehoe,²⁸ S. K. Kim,¹⁰ B. Klima,²³ C. Klopfenstein,¹⁸ W. Ko,¹⁸ J. M. Kohli,⁶ D. Koltick,²⁹ A. V. Kostitskiy,¹⁵ J. Kotcher,⁴³ A. V. Kotwal,³⁹ A. V. Kozelov,¹⁵ E. A. Kozlovsky,¹⁵ J. Krane,³⁸ M. R. Krishnaswamy,⁸ S. Krzywdzinski,²³ S. Kuleshov,¹³ Y. Kulik,⁴² S. Kunori,³³ F. Landry,³⁷ G. Landsberg,⁴⁶ B. Lauer,³⁰ A. Leflat,¹⁴ J. Li,⁴⁷ Q. Z. Li,²³ J. G. R. Lima,³ D. Lincoln,²³ S. L. Linn,²¹ J. Linnemann,³⁷ R. Lipton,²³ F. Lobkowicz,⁴¹ A. Lucotte,⁴² L. Lueking,²³ A. L. Lyon,³³ A. K. A. Maciel,² R. J. Madaras,¹⁷ R. Madden,²¹ L. Magaña-Mendoza,¹¹ V. Manankov,¹⁴ S. Mani,¹⁸ H. S. Mao,^{23,†} R. Markeloff,²⁵ T. Marshall,²⁷ M. I. Martin,²³ K. M. Mauritz,³⁰ B. May,²⁶ A. A. Mayorov,¹⁵ R. McCarthy,⁴² J. McDonald,²¹ T. McKibben,²⁴ J. McKinley,³⁷ T. McMahon,⁴⁴ H. L. Melanson,²³ M. Merkin,¹⁴ K. W. Merritt,²³ C. Miao,⁴⁶ H. Miettinen,⁴⁹ A. Mincer,⁴⁰ C. S. Mishra,²³ N. Mokhov,²³ N. K. Mondal,⁸ H. E. Montgomery,²³ P. Mooney,⁴ M. Mostafa,¹ H. da Motta,² C. Murphy,²⁴ F. Nang,¹⁶ M. Narain,³⁴ V. S. Narasimham,⁸ A. Narayanan,¹⁶ H. A. Neal,³⁶ J. P. Negret,⁴ P. Nemethy,⁴⁰ D. Norman,⁴⁸ L. Oesch,³⁶ V. Oguri,³ N. Oshima,²³ D. Owen,³⁷ P. Padley,⁴⁹ A. Para,²³ N. Parashar,³⁵ Y. M. Park,⁹ R. Partridge,⁴⁶ N. Parua,⁸ M. Paterno,⁴¹ B. Pawlik,¹² J. Perkins,⁴⁷ M. Peters,²² R. Piegaia,¹ H. Piekarczyk,²¹ Y. Pischalnikov,²⁹ B. G. Pope,³⁷ H. B. Prosper,²¹ S. Protopopescu,⁴³ J. Qian,³⁶ P. Z. Quintas,²³ R. Raja,²³ S. Rajagopalan,⁴³ O. Ramirez,²⁴ S. Reucroft,³⁵ M. Rijssenbeek,⁴² T. Rockwell,³⁷ M. Roco,²³ P. Rubinov,²⁶ R. Ruchti,²⁸ J. Rutherford,¹⁶ A. Sánchez-Hernández,¹¹ A. Santoro,² L. Sawyer,³² R. D. Schamberger,⁴² H. Schellman,²⁶ J. Sculli,⁴⁰ E. Shabalina,¹⁴ C. Shaffer,²¹ H. C. Shankar,⁸ R. K. Shivpuri,⁷ D. Shpakov,⁴² M. Shupe,¹⁶ H. Singh,²⁰ J. B. Singh,⁶ V. Sirotenko,²⁵ E. Smith,⁴⁵ R. P. Smith,²³ R. Snihur,²⁶ G. R. Snow,³⁸ J. Snow,⁴⁴ S. Snyder,⁴³ J. Solomon,²⁴ M. Sosebee,⁴⁷ N. Sotnikova,¹⁴ M. Souza,² G. Steinbrück,⁴⁵ R. W. Stephens,⁴⁷ M. L. Stevenson,¹⁷ F. Stichelbaut,⁴³ D. Stoker,¹⁹ V. Stolin,¹³ D. A. Stoyanova,¹⁵ M. Strauss,⁴⁵ K. Streets,⁴⁰ M. Strovink,¹⁷ A. Sznajder,² P. Tamburello,³³ J. Tarazi,¹⁹ M. Tartaglia,²³ T. L. T. Thomas,²⁶ J. Thompson,³³ T. G. Trippe,¹⁷ P. M. Tuts,³⁹ V. Vaniev,¹⁵ N. Varelas,²⁴ E. W. Varnes,¹⁷ A. A. Volkov,¹⁵ A. A. Vorobiev,¹⁵ H. D. Wahl,²¹ G. Wang,²¹ J. Warchol,²⁸ G. Watts,⁴⁶ M. Wayne,²⁸ H. Weerts,³⁷ A. White,⁴⁷ J. T. White,⁴⁸ J. A. Wightman,³⁰ S. Willis,²⁵ S. J. Wimpenny,²⁰ J. V. D. Wirjawan,⁴⁸ J. Womersley,²³ E. Won,⁴¹ D. R. Wood,³⁵ Z. Wu,^{23,†} R. Yamada,²³ P. Yamin,⁴³ T. Yasuda,³⁵ P. Yepes,⁴⁹ K. Yip,²³ C. Yoshikawa,²² S. Youssef,²¹ J. Yu,²³ Y. Yu,¹⁰ B. Zhang,^{23,†} Z. Zhou,³⁰ Z. H. Zhu,⁴¹ M. Zielinski,⁴¹ D. Zieminska,²⁷ A. Zieminski,²⁷ E. G. Zverev,¹⁴ and A. Zylberstejn⁵

(D0 Collaboration)

- ¹Universidad de Buenos Aires, Buenos Aires, Argentina
²LAFEX, Centro Brasileiro de Pesquisas Físicas, Rio de Janeiro, Brazil
³Universidade do Estado do Rio de Janeiro, Rio de Janeiro, Brazil
⁴Universidad de los Andes, Bogotá, Colombia
⁵DAPNIA/Service de Physique des Particules, CEA, Saclay, France
⁶Panjab University, Chandigarh, India
⁷Delhi University, Delhi, India
⁸Tata Institute of Fundamental Research, Mumbai, India
⁹Kyungshung University, Pusan, Korea
¹⁰Seoul National University, Seoul, Korea
¹¹CINVESTAV, Mexico City, Mexico
¹²Institute of Nuclear Physics, Kraków, Poland
¹³Institute for Theoretical and Experimental Physics, Moscow, Russia
¹⁴Moscow State University, Moscow, Russia
¹⁵Institute for High Energy Physics, Protvino, Russia
¹⁶University of Arizona, Tucson, Arizona 85721
¹⁷Lawrence Berkeley National Laboratory and University of California, Berkeley, California 94720
¹⁸University of California, Davis, California 95616
¹⁹University of California, Irvine, California 92697
²⁰University of California, Riverside, California 92521
²¹Florida State University, Tallahassee, Florida 32306
²²University of Hawaii, Honolulu, Hawaii 96822
²³Fermi National Accelerator Laboratory, Batavia, Illinois 60510
²⁴University of Illinois at Chicago, Chicago, Illinois 60607
²⁵Northern Illinois University, DeKalb, Illinois 60115
²⁶Northwestern University, Evanston, Illinois 60208
²⁷Indiana University, Bloomington, Indiana 47405
²⁸University of Notre Dame, Notre Dame, Indiana 46556
²⁹Purdue University, West Lafayette, Indiana 47907
³⁰Iowa State University, Ames, Iowa 50011
³¹University of Kansas, Lawrence, Kansas 66045
³²Louisiana Tech University, Ruston, Louisiana 71272
³³University of Maryland, College Park, Maryland 20742
³⁴Boston University, Boston, Massachusetts 02215
³⁵Northeastern University, Boston, Massachusetts 02115
³⁶University of Michigan, Ann Arbor, Michigan 48109
³⁷Michigan State University, East Lansing, Michigan 48824
³⁸University of Nebraska, Lincoln, Nebraska 68588
³⁹Columbia University, New York, New York 10027
⁴⁰New York University, New York, New York 10003
⁴¹University of Rochester, Rochester, New York 14627
⁴²State University of New York, Stony Brook, New York 11794
⁴³Brookhaven National Laboratory, Upton, New York 11973
⁴⁴Langston University, Langston, Oklahoma 73050
⁴⁵University of Oklahoma, Norman, Oklahoma 73019
⁴⁶Brown University, Providence, Rhode Island 02912
⁴⁷University of Texas, Arlington, Texas 76019
⁴⁸Texas A&M University, College Station, Texas 77843
⁴⁹Rice University, Houston, Texas 77005

(Received 18 November 1998; revised manuscript received 25 January 1999)

A search has been carried out for events in the channel $p\bar{p} \rightarrow \gamma\gamma + 2 \text{ jets}$. Such a signature can characterize the production of a nonstandard Higgs boson together with a W or Z boson. We refer to this nonstandard Higgs, having standard model couplings to vector bosons but no coupling to fermions, as a “bosonic Higgs.” With the requirement of two high transverse energy photons and two jets, the diphoton mass ($m_{\gamma\gamma}$) distribution is consistent with expected background. A 90 (95)% confidence level (C.L.) upper limit on the cross section as a function of mass is calculated, ranging from 0.60 (0.80) pb for $m_{\gamma\gamma} = 65 \text{ GeV}/c^2$ to 0.26 (0.34) pb for $m_{\gamma\gamma} = 150 \text{ GeV}/c^2$, corresponding to a 95% C.L. lower limit on the mass of a bosonic Higgs of $78.5 \text{ GeV}/c^2$. [S0031-9007(99)08651-2]

PACS numbers: 13.85.Qk, 12.60.Fr, 14.80.Cp

The Higgs sector of the standard model is poorly constrained. Several extended Higgs models [1–6] allow a light neutral scalar Higgs with suppressed couplings to fermions. We refer to such a nonstandard Higgs, having standard model couplings to vector bosons but zero couplings to fermions, as a “bosonic Higgs.” The model of Refs. [1,2] provides a bosonic Higgs without requiring fine-tuning and maintains the relation $\rho = M_W^2/M_Z^2 \cos^2 \theta_W = 1$, consistent with present experimental limits [7].

The decay channels of a bosonic Higgs differ from those of the standard model Higgs as shown in Fig. 1. Since the fermion decay channels are suppressed, the decay of a bosonic Higgs with mass less than $2M_W$ is not dominated by $H \rightarrow b\bar{b}$. At tree level the bosonic Higgs decays only to $WW^{(*)}$ and $ZZ^{(*)}$ vector bosons (where the asterisks denote that one or both of the vector bosons may be off the mass shell). For bosonic Higgs masses less than $90 \text{ GeV}/c^2$, the one-loop W -boson-mediated $H \rightarrow \gamma\gamma$ channel becomes dominant.

A bosonic Higgs is most easily detected in the associated production mode, where an off-mass-shell W or Z boson is produced and radiates a Higgs boson [8]. Higgs production through vector boson fusion also contributes to the $\gamma\gamma + 2 \text{ jets}$ ($\gamma\gamma jj$) final state at the 15% level. The sum of the WH and ZH production cross sections ranges from 1.8 pb for $M_H = 60 \text{ GeV}/c^2$ to 0.4 pb for $M_H = 100 \text{ GeV}/c^2$. We expect sensitivity in the $\gamma\gamma jj$ final state up to a mass of $M_H \sim 85 \text{ GeV}/c^2$ for the decay modes $H \rightarrow \gamma\gamma$ and $W/Z \rightarrow jj$, at which mass the

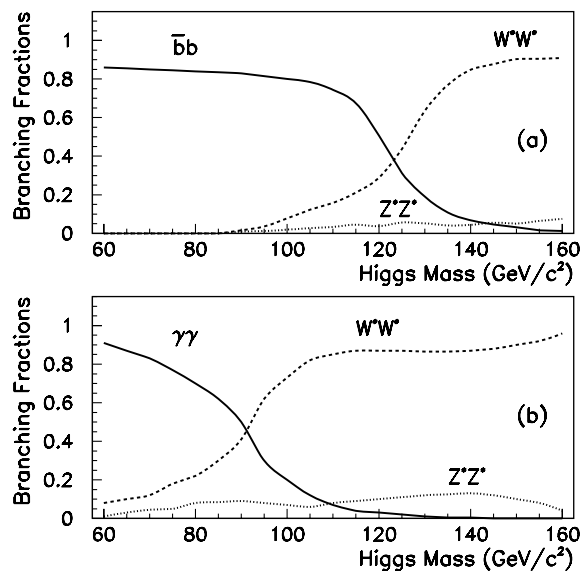


FIG. 1. Decay branching fractions vs Higgs mass for (a) standard model Higgs and (b) bosonic Higgs. In (a), the diphoton branching fraction is less than 0.001; $c\bar{c}$ and $\tau^+\tau^-$ Higgs decay channels are not shown. In (b), the Higgs decays to only VV , where $V = \gamma, W$, or Z . There is a large enhancement in the diphoton channel for the bosonic Higgs model: the absence of competing decay channels results in a dominant $H \rightarrow \gamma\gamma$ below $M_H \approx 90 \text{ GeV}/c^2$.

branching ratio $H \rightarrow \gamma\gamma$ remains high and the falling Higgs production cross section of $\sim 0.4 \text{ pb}$ allows the production of tens of events. This Letter describes the first search for a bosonic Higgs at hadron colliders.

Experiments at the CERN Large Electron-Positron Collider (LEP) have previously set lower mass limits on a bosonic Higgs. A limit of approximately $60 \text{ GeV}/c^2$ was established [8,9] in data taken at the Z^0 , a higher 95% confidence level (C.L.) limit set at $76.5 \text{ GeV}/c^2$ in 172 GeV collisions [10] at LEP2, and this limit extended to $90.0 \text{ GeV}/c^2$ in 183 GeV collisions [11].

Data corresponding to an integrated luminosity of $101.2 \pm 5.5 \text{ pb}^{-1}$, recorded during 1992–1996 with the D0 detector [12], are used for this analysis. Photons and jets are identified using the uranium-liquid-argon sampling calorimeter, extending to a pseudorapidity $|\eta| = |-\ln \tan \frac{\theta}{2}| \leq 4.5$, where θ is the polar angle. The electromagnetic (EM) energy resolution is $\sigma_E/E = 15\%/\sqrt{E(\text{GeV})} \oplus 0.3\%$, and the jet energy resolution is about $\sigma_E/E = 80\%/\sqrt{E(\text{GeV})}$. The calorimeter is segmented transversely into towers in pseudorapidity and azimuthal angle of size $\Delta\eta \times \Delta\phi = 0.1 \times 0.1$ and further segmented to 0.05×0.05 at the EM shower maximum. Drift chambers in front of the calorimeter are used to distinguish photons from electrons. A three-level triggering system is employed: level 0 uses scintillation counters near the beam pipe at each end of the detector to detect an inelastic interaction, level 1 sums the EM and hadronic energy in calorimeter towers of size $\Delta\eta \times \Delta\phi = 0.2 \times 0.2$, and level 2 is a software trigger which forms clusters of calorimeter cells and applies loose cuts on the shower shape.

Events used in this analysis have at least two photon candidates and at least two jet candidates. Initially, the events are selected using a diphoton trigger that requires two EM showers with a transverse energy (E_T) greater than 12 GeV. The filter is fully efficient when both photons have $E_T > 15 \text{ GeV}$. The off-line event selection criteria are optimized by requiring one photon to have $E_T^\gamma > 30 \text{ GeV}$ and $|\eta^\gamma| < 1.1$ or $1.5 < |\eta^\gamma| < 2.0$, and the other to have $E_T^\gamma > 15 \text{ GeV}$ and $|\eta^\gamma| < 1.1$ or $1.5 < |\eta^\gamma| < 2.25$. Additionally, one hadronic jet is required to have $E_T^{\text{jet}} > 30 \text{ GeV}$ and $|\eta^{\text{jet}}| < 2.0$, and the other hadronic jet is required to have $E_T^{\text{jet}} > 15 \text{ GeV}$ and $|\eta^{\text{jet}}| < 2.25$. For the two jets to be consistent with the decay of a W or Z boson, the dijet mass is required to be between 40 and $150 \text{ GeV}/c^2$. A photon candidate is rejected if there is either a reconstructed track or a significant number of drift chamber hits in a tracking road $\Delta\theta \times \Delta\phi = 0.2 \times 0.2$ between the cluster in the calorimeter and the interaction vertex. A photon candidate is required to have a shower shape consistent with that of a single EM shower, to have more than 96% of its energy in the EM section of the calorimeter, and to be isolated [13]. Isolation requires that the transverse energy in the annular region between $\mathcal{R} \equiv \sqrt{\Delta\eta^2 + \Delta\phi^2} = 0.2$

and $\mathcal{R} = 0.4$ around the cluster be less than 10% of the total cluster transverse energy. In addition, each photon candidate must be separated by $\Delta\mathcal{R}_\gamma > 0.7$ from every jet [14]. Each jet candidate is reconstructed from energy deposited in a $\Delta\mathcal{R} < 0.7$ cone, must have less than 95% of its energy in the EM section of the calorimeter, and must have no more than 40% of its energy in the outermost layer of the hadronic portion of the calorimeter.

These selection criteria yield four events, whose $m_{\gamma\gamma}$ distribution is shown in Fig. 2a. No events are observed with $m_{\gamma\gamma} > 60 \text{ GeV}/c^2$. The resolution of the detector in $m_{\gamma\gamma}$ is about $2.5 \text{ GeV}/c^2$ for diphoton final states passing these kinematic cuts. The corresponding dijet mass distributions of data and expected background are shown in Fig. 2b.

The dominant background to the $\gamma\gamma jj$ channel is production of QCD multijet events in which two jets are misidentified as photons. During the jet fragmentation process, π^0 and η mesons are produced and decay promptly into multiple photons. If the π^0 or η meson carries a large fraction of the jet energy and has a momentum greater than about $10 \text{ GeV}/c$ the decay photons coalesce to mimic a single isolated photon in the calorimeter. The depth development of multiple photons differs from that of a single photon, and a fit to the longitudinal shower shape for photon candidates yields the probability $P(j \rightarrow \gamma)$ for a jet to mimic an isolated photon candidate, estimated to be $(4.3 \pm 1.0) \times 10^{-4}$, with a weak E_T dependence [14].

Smaller sources of background are from double direct photon production, single direct photon production with one jet fluctuating into a photon candidate, and final states containing electrons in addition to two jets, such as ($W \rightarrow e^\pm \nu$) γjj , ($Z \rightarrow e^+ e^-$) jj , and $t\bar{t} \rightarrow e^+ e^- \nu \nu jj$, where the electrons fail track reconstruction and are

misidentified as photons. By rejecting events that have a track or significant number of drift chamber hits inside the tracking road, the expected electron background is reduced to less than 0.01 events and is not considered further.

The QCD multijet background to $\gamma\gamma jj$ events is estimated from the data. Starting with the same trigger and data set as the signal sample, a background sample is selected by requiring two EM clusters and jets satisfying the same kinematic and fiducial criteria as the signal. Both EM clusters are required to have more than 90% of their energy in the EM section of the calorimeter and to have no reconstructed track associated with the cluster, but at least one of the two EM clusters is required to fail the photon quality criteria (isolation, shower shape, or EM fraction). The resulting sample of 194 events is expected to be dominated by QCD multijet events where two jets fluctuate into highly electromagnetic clusters. After subtracting the expected direct photon event contribution, the QCD multijet background for $m_{\gamma\gamma} > 60 \text{ GeV}/c^2$ is estimated by normalizing the cluster-pair mass distribution to the signal sample over the mass range $m_{\gamma\gamma} < 60 \text{ GeV}/c^2$, where bosonic Higgs have been excluded by earlier searches for $Z \rightarrow Z^* H$ at LEP [9,10].

The direct photon background is calculated using the PYTHIA Monte Carlo program [15]. This background has two sources: single direct photon production, where one true photon is produced and one jet is misidentified as a photon, and double direct photon production, where two true photons are produced in addition to two high- E_T jets. The Monte Carlo jet and photon energies are smeared to match the measured detector resolutions. The efficiency for the events to pass the photon quality criteria (isolation, shower shape, EM fraction, and tracking) are calculated from data using our $Z \rightarrow e^+ e^-$ event sample. The single direct photon events are weighted by the probability $P(j \rightarrow \gamma)$, since one of the jets must be misidentified as a photon for a background event to be accepted. The direct photon background is normalized to the signal sample using the calculated direct photon cross section. The dominant systematic uncertainty in these sources of background then derives from the observed level of agreement between the theoretical and experimental direct photon cross sections and is estimated to be 40% for double direct photon production and 20% for single direct photon production [13,16].

Figure 2 shows the total expected background, with estimated uncertainties, in bins of $10 \text{ GeV}/c^2$. The total background of 6.0 ± 1.6 events consists of 4.0 ± 1.5 QCD multijet events and 2.0 ± 0.6 direct photon events. It agrees well with our observed number of four events. We find no evidence for nonstandard sources of $\gamma\gamma jj$ events. If we increase the photon pseudorapidity coverage to $|\eta^\gamma| < 2.5$ and reduce the leading jet and photon transverse energy requirements to 15 GeV , the same background estimation technique predicts 38 ± 10 events while 39 events are observed. The $m_{\gamma\gamma}$ and m_{jj}

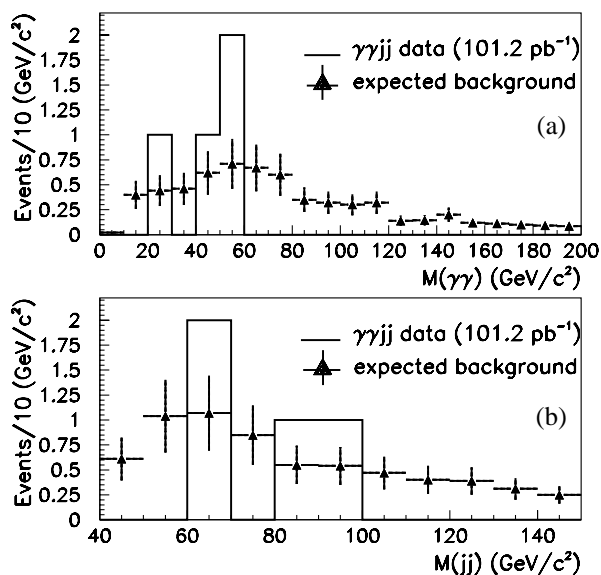


FIG. 2. The data and expected background for (a) the diphoton mass and (b) the dijet mass distributions.

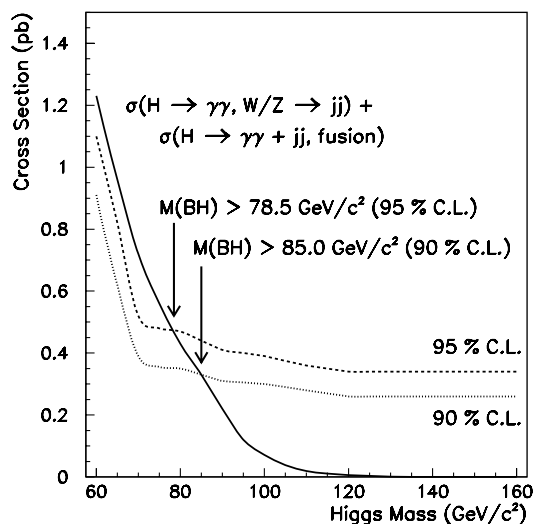


FIG. 3. The solid curve represents the bosonic Higgs 95% C.L. exclusion contour, the dashed curve represents the 90% C.L. exclusion contour, and the dotted curve represents the bosonic Higgs cross section with $H \rightarrow \gamma\gamma$ and $W/Z \rightarrow jj$ branching fractions taken into account.

distributions of this larger sample are also described well by the estimated background.

Seven samples of bosonic Higgs events, each containing 5000 simulated events, are generated using PYTHIA for the processes $p\bar{p} \rightarrow WH$ and $p\bar{p} \rightarrow ZH$, with the decays $H \rightarrow \gamma\gamma$ and $W/Z \rightarrow qq'$, for Higgs masses of 60, 70, 80, 90, 100, 110, and 150 GeV/c^2 . These events are processed through the detector simulation and event reconstruction software. The Higgs selection criteria are applied and the signal acceptance and efficiency calculated; their product ranges from 0.06 to 0.10 for Higgs masses of 60 to 150 GeV/c^2 . The systematic uncertainty in the acceptance for the Higgs signal is based on the level of agreement between the Monte Carlo and data-based estimates of the photon and jet selection efficiencies. The systematic error includes the uncertainties in the efficiencies for the photon trigger and selection (2%), requirement on photon track rejection (13%), hadronic energy scale (5%–11%), EM energy scale ($\approx 1\%$), and jet reconstruction ($\approx 1\%$). The statistical uncertainty on the Monte Carlo Higgs samples is about 3%. The systematic and statistical uncertainties, and the integrated luminosity uncertainty of 5.3%, are added in quadrature and yield 15%.

The 90% and 95% confidence level limits on the cross section as a function of $m_{\gamma\gamma}$ are shown in Fig. 3 and are calculated using a Bayesian approach [7], incorporating the uncertainties associated with the efficiency, acceptance, luminosity, and the expected background as a function of $m_{\gamma\gamma}$ and m_{jj} . Correlations between errors are negligible and not included. A general 95% C.L. upper limit on the cross section is calculated from the exclusion contour in Fig. 3 and ranges from 0.80 pb for $m_{\gamma\gamma} = 65 \text{ GeV}/c^2$ to 0.34 pb for $m_{\gamma\gamma} = 150 \text{ GeV}/c^2$. The corresponding 90% C.L. is noted in the figure. The full bosonic Higgs cross section is also plotted in Fig. 3

and includes both the associated production and vector boson fusion production processes, calculated using PYTHIA with a QCD correction factor [8] of 1.25. This factor agrees with the ratio between our measured cross section for W boson production [17] and the calculated cross section, 1.23 ± 0.08 . We set lower limits on the bosonic Higgs mass of $85.0 \text{ GeV}/c^2$ at the 90% C.L. and $78.5 \text{ GeV}/c^2$ at the 95% C.L.

In summary, we performed the first search for a bosonic Higgs at hadron colliders, in the channel $p\bar{p} \rightarrow \gamma\gamma jj$. Four candidates pass the selection requirements, with an expected background of 6.0 ± 2.1 events. No candidate events are seen with a diphoton mass greater than $60 \text{ GeV}/c^2$. A 95% C.L. bosonic Higgs lower mass limit of $78.5 \text{ GeV}/c^2$ is set, assuming standard model couplings between the Higgs and the vector bosons. The 95% C.L. upper limits on the bosonic Higgs production cross section range from 0.80 pb for $m_{\gamma\gamma} = 65 \text{ GeV}/c^2$ to 0.34 pb for $m_{\gamma\gamma} = 150 \text{ GeV}/c^2$.

We thank the staffs at Fermilab and collaborating institutions for their contributions to this work, and we acknowledge support from the Department of Energy and National Science Foundation (U.S.A.), Commissariat à l'Énergie Atomique (France), Ministry for Science and Technology and Ministry for Atomic Energy (Russia), CAPES and CNPq (Brazil), Departments of Atomic Energy and Science and Education (India), Colciencias (Colombia), CONACyT (Mexico), Ministry of Education and KOSEF (Korea), and CONICET and UBACyT (Argentina).

*Visitor from Universidad San Francisco de Quito, Quito, Ecuador.

†Visitor from IHEP, Beijing, China.

- [1] A. G. Akeroyd, Phys. Lett. B **368**, 89 (1996).
- [2] A. G. Akeroyd, Phys. Lett. B **353**, 519 (1995).
- [3] H. E. Haber, G. L. Kane, and T. Sterling, Nucl. Phys. **B161**, 493 (1979).
- [4] H. Pois, T. Weiler, and T. C. Yuan, Phys. Rev. D **47**, 3886 (1993).
- [5] P. Bamert and Z. Kunszt, Phys. Lett. B **306**, 335 (1993).
- [6] H. Georgi and M. Machacek, Nucl. Phys. **B262**, 463 (1985); M. Chanowitz and M. Golden, Phys. Lett. **165B**, 105 (1985).
- [7] R. M. Barnett *et al.*, Phys. Rev. D **54**, 1 (1996).
- [8] A. Stange, W. Marciano, and S. Willenbrock, Phys. Rev. D **49**, 1354 (1994).
- [9] L3 Collaboration, M. Acciarri *et al.*, Phys. Lett. B **388**, 409 (1996).
- [10] OPAL Collaboration, K. Ackerstaff *et al.*, Eur. Phys. J. C **1**, 31 (1998).
- [11] OPAL Collaboration, K. Ackerstaff *et al.*, Phys. Lett. B **437**, 218 (1998).
- [12] D0 Collaboration, S. Abachi *et al.*, Nucl. Instrum. Methods Phys. Res., Sect. A **338**, 185 (1994).
- [13] D0 Collaboration, S. Abachi *et al.*, Phys. Rev. Lett. **78**, 2070 (1997).

-
- [14] Bryan A. Lauer, Ph.D. thesis, Iowa State University, Ames, IA, 1997, available at http://www-d0.fnal.gov/results/publications_talks/thesis/lauer/thesis.ps (unpublished).
- [15] T. Sjostrand and M. Bengtsson, *Comput. Phys. Commun.* **43**, 367 (1987). Version 5.7 was used in this analysis.
- [16] W. Chen, Ph.D. thesis, State University of New York, Stony Brook, NY, 1997, available at http://www-d0.fnal.gov/results/publications_talks/thesis/chen/chen.html (unpublished).
- [17] D0 Collaboration, S. Abachi *et al.*, *Phys. Rev. Lett.* **75**, 1456 (1995).